Realization of the kicked atom

M. T. Frey* and F. B. Dunning
Department of Physics and the Rice Quantum Institute, Rice University, 6100 South Main Street, Houston, Texas 77005-1892

C. O. Reinhold, S. Yoshida, and J. Burgdörfer†
Physics Division, Oak Ridge National Laboratory, Oak Ridge, Tennessee 37831-6377
and Department of Physics, University of Tennessee, Knoxville, Tennessee 37996-1200

(Received 8 July 1998)

The kicked atom is realized experimentally by exposing potassium np Rydberg atoms with $n \sim 388$ to a sequence of up to 50 half-cycle pulses whose duration is much shorter than the classical electron orbital period. The Rydberg atom survival probability is observed to have a broad maximum for pulse repetition frequencies near the classical orbital frequency. Comparisons with detailed classical trajectory Monte Carlo simulations show that this behavior provides an unambiguous signature of dynamical stabilization. The classical simulations further show that the kicked hydrogen atom is, depending on the pulse repetition frequency, chaotic or characterized by a mixed phase space with various families of fully stable islands within which the atom is stable against ionization. Signatures of stabilization and chaotic diffusion are also observed in the final bound-state distribution of the surviving atoms. [S1050-2947(99)07302-3]

PACS number(s): 42.50.Hz, 32.80.Rm, 03.65.Bz

I. INTRODUCTION

Periodically ''kicked'' systems, i.e., impulsively driven systems where the duration of each impulse is short compared to the period of the unperturbed system, provide valuable test cases for the study of nonlinear dynamics in Hamiltonian systems. Prime examples are the kicked rotor (or standard map [1]) and the kicked hydrogen atom [2–9]. The time evolution for kicked systems can be reduced to a sequence of discrete maps between adjacent kicks. This simplification permits detailed numerical studies of the long-term evolution using both classical and quantum dynamics, and hence, of the classical-quantum correspondence in microscopic systems that feature regular and chaotic dynamics. While systems subject to sinusoidal perturbations have been widely studied, for example hydrogen in a microwave field [10,11], experimental realizations of kicked systems have been scarce. Recently, however, atoms cooled in a standing light wave have provided a realization of the one-dimensional standard map, demonstrating the existence of Anderson localization in the translational motion of a single atom [12,13].

Atoms in which an electron is excited to a state of large principal quantum number n also afford the opportunity to study the behavior of kicked systems because the classical orbital period T_n of the excited electron is very large (~ 10 ns at $n=400$ increasing to ~ 150 ns at $n=1000$). It is therefore possible using conventional pulse generators to apply unidirectional electric field pulses, termed half-cycle pulses (HCPs), to such atoms whose duration T_p is much shorter than the orbital period [14–16]. In the limit that $T_p/T_n \ll 1$, a single pulse, $\vec{F}_{\mathrm{HCP}}(t)$, simply delivers an impulsive momentum transfer or ''kick,''

$$\Delta \vec{p} = -\int \vec{F}_{\mathrm{HCP}}(t)\,dt, \tag{1}$$

to the excited electron, where atomic units are used throughout. Thus, very high-n atoms that are subject to a periodic sequence of HCPs provide an ideal testing ground to examine the behavior of kicked systems.

The impulsively driven (kicked) Rydberg atom has been the focus of a number of theoretical investigations [2–9], many of which have considered trains of impulses that alternate in sign. Such a sequence of impulses has been used to model atoms in a monochromatic radiation field and has provided, for example, new insights into intense-field stabilization [8,9,17–19]. The behavior of a hydrogen atom subject to a series of unidirectional kicks has been investigated within a one-dimensional (1D) model [6]. Fully developed classical chaos was observed, and the bound portion of the phase space was found to decay algebraically as a function of time as $\sim t^{-1.65}$. Little is known about the response of a three-dimensional (3D) Rydberg atom to a train of unidirectional pulses.

In this work we show both experimentally and theoretically that the phase space of the kicked atom contains sizable regular islands that give rise to dynamical stabilization. (A preliminary account of our findings was given in [20].) Experimental measurements of the survival probability versus HCP repetition frequency are presented which reveal a pronounced structure that is well reproduced by classical trajectory Monte Carlo (CTMC) simulations. Calculations were undertaken for potassium and for hydrogen in three and one dimensions. The 1D model gives results that closely parallel those for the 3D system and allows detailed examination of the stabilization in terms of the mixed phase-space structure.

*Present address: Schlumberger Sugar Land Products Center, P.O. Box 2175, Houston, TX 77252-2175.

†Present address: Institute for Theoretical Physics, Vienna University of Technology, A-1040 Vienna, Austria.

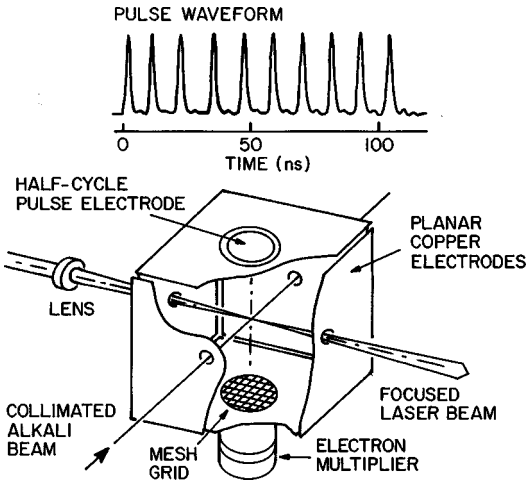

FIG. 1. Schematic diagram of the apparatus. The inset shows a typical profile of the train of HCPs used in this work.

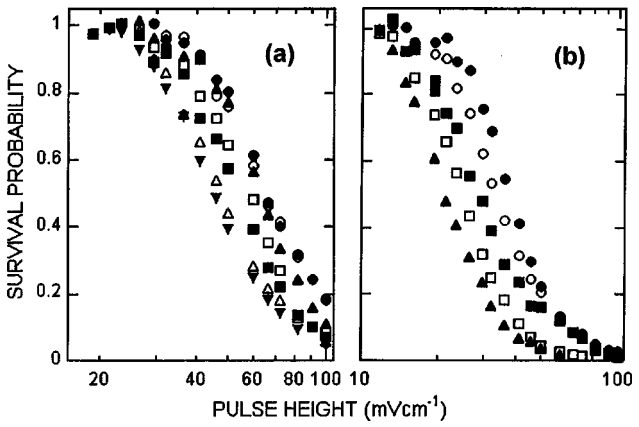

FIG. 2. Measured survival probability of K(np) atoms with $n \sim 388$ as a function of the pulsed field amplitude following application of (a) 10 HCPs with pulse repetition frequencies of 227 MHz (solid circles), 200 MHz (open circles), 125 MHz (solid triangles), 100 MHz (open squares), 83 MHz (solid squares), 50 MHz (open triangles), and 10 MHz (inverted solid triangles) and (b) 50 HCPs with pulse frequencies of 250 MHz (solid circles), 166 MHz (open circles), 100 MHz (solid squares), 50 MHz (open squares), and 20 MHz (solid triangles).

Signatures of stabilization and of chaotic diffusion are also found in the final bound-state distribution, as measured by selective field ionization.

II. EXPERIMENTAL REALIZATION OF THE KICKED ATOM

In order to realize a kicked system in the laboratory, potassium Rydberg atoms with $n \sim 388$ are exposed to a train of equispaced unidirectional HCPs, each having a duration $T_p \simeq 2$ ns. For $n \sim 388$, the atomic orbital period T_n is $\simeq 9$ ns and the condition $T_p/T_n \ll 1$ is satisfied. Application of such pulse trains can lead to ionization. The Rydberg atom survival probability is measured as a function of the number, amplitude, and repetition frequency of the pulses using the apparatus shown in Fig. 1. The Rydberg atoms are created by photoexciting ground-state potassium atoms in a tightly collimated thermal-energy beam using a frequency-stabilized, intracavity-doubled Coherent CR 699-21 Rh6G dye laser. Excitation occurs near the center of an interaction region defined by three pairs of planar electrodes, each 10×10 cm. The use of large electrodes well separated from the experimental volume minimizes the effect of patch fields associated with nonuniformities in the electrode surfaces. However, even with all electrodes grounded, fields of ~ 2 mV cm^{-1} remain in the experimental volume. These are locally reduced to $\lesssim 50$ μV cm^{-1} by application of small bias potentials to the electrodes that are determined using a technique based on the Stark effect. To minimize motional electric fields, the magnetic field is reduced to $\lesssim 20$ mG by use of μ-metal shields.

Measurements are conducted in a pulsed mode. The laser output is formed into a train of pulses of ~ 4 μs duration and ~ 10 kHz pulse repetition frequency using an acousto-optic modulator. (The probability that a Rydberg atom is formed during a laser pulse is very small, $\lesssim 0.05$, and data must be accumulated following many laser pulses.) Excitation occurs in (near) zero electric field. Approximately 200 ns after each laser pulse, the atoms are subject to a train of HCPs generated by applying voltage pulses to a circular electrode 4 cm in diameter that is inset in the upper plate. The pulse shapes and amplitudes are measured directly at the circular electrode using a fast probe and sampling oscilloscope. A typical pulse train is included in Fig. 1. The number and excited state distribution of Rydberg atoms remaining in the experimental volume after application of the HCPs is measured after a time delay of ~ 6 μs, using selective field ionization (SFI). The time delay discriminates against free low-energy electrons resulting from HCP-induced ionization which, tests revealed, have a residence time of ~ 5 μs in the interaction region. For SFI, a slowly varying (~ 1 μs rise time) voltage ramp is applied to the bottom interaction-region electrode. Electrons resulting from field ionization are accelerated to, and detected by, a particle multiplier. Because atoms in different Rydberg states ionize at different applied fields, measurement of the field ionization signal as a function of time, i.e., of applied field, provides a measure of the excited-state distribution of those atoms present at the time of application of the ramp. Measurements in which no HCPs are applied are interspersed at routine intervals during data acquisition to monitor the number of Rydberg atoms initially created by the laser. The Rydberg atom survival probability is determined by taking the ratio of the Rydberg atom signals observed with and without HCP application.

Survival probabilities measured following application of trains of ten and fifty equispaced HCPs are presented in Figs. 2(a) and 2(b), respectively, as a function of HCP amplitude for several values of the pulse repetition frequency. As might be expected, significantly larger HCP heights are required to induce ionization with ten HCPs than with fifty HCPs. More surprising and important, however, is the observation that for a given HCP amplitude the survival probability depends markedly on the repetition frequency ν_T of the HCPs in the train. This is better illustrated in Fig. 3, which shows the Rydberg atom survival probability following application of ten and fifty HCPs with peak fields of 29 and 60 mV cm^{-1} as a function of ν_T, expressed in MHz and in scaled units. Here, and in the following, scaled units will be used to explicitly display the scaling invariance of the classical dynam-

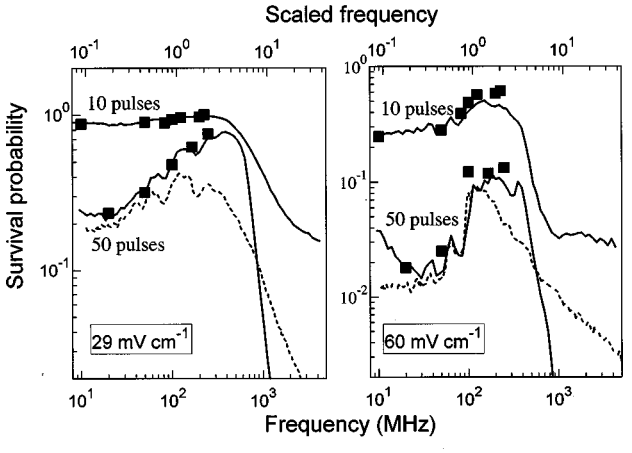

FIG. 3. Rydberg atom survival probability following application of ten and fifty HCPs with peak fields of 29 mV/cm and 60 mV/cm as a function of the HCP repetition frequency. Experimental data, □; results of CTMC calculations for K($388p$), ——; CTMC results for the impulsively driven H($388p$) atom with $n_i\Delta p=0.3$, — — —. The HCP repetition frequency is displayed in MHz and in scaled units $\nu_0=\nu_T 2\pi n_i^3$.

ics of the Rydberg-Coulomb orbits. Classically, all energy levels are equivalent in that they can be mapped onto each other by the following scaling transformation [21] for coordinates, momenta, time, frequency, and momentum transfer, respectively:

$$q\rightarrow n^2 q, \tag{2}$$

$$p\rightarrow n^{-1}p, \tag{3}$$

$$t\rightarrow n^3 t, \tag{4}$$

$$\nu_n\rightarrow n^{-3}\nu_n, \tag{5}$$

$$\Delta p\rightarrow n^{-1}\Delta p, \tag{6}$$

where n is the scaling parameter which is equivalent to the classical action in units of $\hbar$ (i.e., the principal quantum number). Figure 3 reveals a broad maximum in the survival probability for pulse repetition frequencies near the classical orbital frequency, precisely the regime in which dynamical stabilization of the kicked atom might be expected.

To investigate the origin of the maximum in the survival probability, a series of CTMC calculations were undertaken using the Hamiltonian

$$H(t)=H_{\rm at}+zF(t)\simeq H_{\rm at}+\sum_{j=1}^{N} zF_{\rm HCP}(t-j\nu_T^{-1}), \tag{7}$$

where $F_{\rm HCP}$ is the field of a single pulse. We fit the experimental profile $F(t)$ to a periodic train of individual pulses which, strictly speaking, becomes valid only after the first two pulses. The atomic Hamiltonian is given by

$$H_{\rm at}=\frac{p^2}{2}+V_{\rm at}(r) \tag{8}$$

$$=\frac{p_z^2+p_\rho^2}{2}+\frac{L_z^2}{2\rho^2}+V_{\rm at}(\sqrt{z^2+\rho^2}). \tag{9}$$

We use a one-electron model potential $V_{\rm at}$ for the K^+ core potential that yields accurate quantum defects and satisfies the correct boundary conditions at small and large distances. The time evolution of the electron is modeled using a quasiclassical approach in which the wave function is replaced by a classical probability density in phase space, $f(\vec{r},\vec{p},t)$. Formally, the time evolution of this density is governed by the classical Liouville equation for the Hamiltonian $H(t)$ [Eq. (7)],

$$\frac{\partial f}{\partial t}=[H,f], \tag{10}$$

where [,] denotes a Poisson bracket. Since classical phase-space points evolve in time independently according to Hamilton's equations, the Liouville equation can be easily solved using a Monte Carlo technique. The resulting method is usually referred to as the classical trajectory Monte Carlo (CTMC) approach [22].

The experimental conditions for preparation of potassium Rydberg atoms are such that $\ell=1$ states with a statistical population of m substates are produced. Within the CTMC approach, this initial quantum state can be modeled by a subset of a microcanonical ensemble

$$f_i(\vec{r},\vec{p})=C_i\delta\left[E_i-\frac{p^2}{2}-V_{\rm at}(r)\right]\Theta(L-\ell)\Theta(\ell+1-L), \tag{11}$$

where C_i is a normalization constant, E_i is the initial quantum mechanical binding energy, and Θ denotes a step function.

Calculated survival probabilities are included in Fig. 3 and display excellent agreement with the experimental data without recourse to any adjustable parameters. This agreement indicates that the stabilization signaled by the increased survival probability for $\nu_0\gtrsim 1$ is classical in origin. Similarly, good agreement is obtained if a Coulomb potential is used for $V_{\rm at}$. Note that in the limit of high frequencies the train of pulses becomes equivalent to a single pulse, $F(t)\simeq NF_{HCP}(t)$, for which the agreement between the theory and experiment (not shown here) is well established [16].

Because the Hamilton equations for finite-width pulses must be solved numerically, it is not computationally feasible to investigate the long-term stability in the limit $N\rightarrow\infty$ (typically $N\gtrsim 10^6$) and to perform a detailed analysis of the classical phase space. Thus, to further examine the origin of the maximum observed in the survival probability, we have also performed calculations for the ''kicked'' hydrogen atom (i.e., assuming the sudden limit in which each HCP can be replaced by a δ-function impulse), details of which are given in the next sections. Results for the survival probability within this model are also given in Fig. 3. This simplified model reproduces the observed overall structure in the survival probability although the stability is somewhat reduced. This results because the finite width of each experimental HCP cuts off the higher frequencies in the perturbation

which enhances the stability of the orbit. The similarities between the different calculations and the experiment suggest that the stabilization can be analyzed in detail in terms of the ''kicked'' atom. In the following, we analyze theoretically the dynamics of the simplest system, the 1D kicked atom, and we discuss the conditions for which the evolution of the electron is regular or chaotic. Subsequently, we show that similar situations can be found for the 3D kicked atom.

III. ONE-DIMENSIONAL KICKED ATOM

Consider the electron in a 1D hydrogen ''atom'' that is subject to a periodic train of impulses Δp with frequency ν_T (period T_T). The dynamics of the atom is governed by the Hamiltonian

$$H^{1D}(q,p,t)=H_{at}^{1D}(q,p)-q\Delta p\sum_{k=1}^{N}\delta(t-k/\nu_T) \tag{12}$$

$$=\frac{p^2}{2}+\frac{\Lambda^2}{2q^2}-\frac{1}{q}-q\Delta p\sum_{k=1}^{N}\delta(t-k/\nu_T), \tag{13}$$

where q and p denote the position and momentum of the electron. The 1D atom is described by an unperturbed Hamiltonian H_{at}^{1D} and includes an effective centrifugal barrier with quasi-angular momentum Λ. We take the limit $\Lambda\rightarrow 0$ and, therefore, the only role of this potential is to provide an infinite barrier at $q=0$ such that the motion is confined to the $q>0$ region of phase space.

Denoting the phase-space coordinates just before the kth kick by (q_k,p_k), the time evolution during a single period of the perturbation is given by a map of phase-space coordinates,

$$(q_k,p_k)=M(q_{k-1},p_{k-1})=M_{\mathrm{Coul}}\circ M_{\Delta p}(q_{k-1},p_{k-1}), \tag{14}$$

where $M_{\Delta p}$ describes the kick, i.e.,

$$(q_{k-1},p_{k-1}+\Delta p)=M_{\Delta p}(q_{k-1},p_{k-1}), \tag{15}$$

and M_{Coul} describes the unperturbed Coulomb evolution governed by H_{at}^{1D}. The latter depends on the atomic energies $E_k=H_{at}^{1D}(q_k,p_k)$. Note that only $M_{\Delta p}$ changes the atomic energy according to

$$E_k=ME_{k-1}=M_{\Delta p}E_{k-1}=\frac{(\Delta p)^2}{2}+p_{k-1}\Delta p+E_{k-1}. \tag{16}$$

Using the parametric form of Coulomb orbits [21], the full mapping M for $E_k<0$ is given by a set of implicit equations:

$$q_{k-1}=n_k^2(1-\epsilon_k\cos\xi_{k-1}),$$

$$p_{k-1}+\Delta p=\frac{n_k}{q_{k-1}}\epsilon_k\sin\xi_{k-1},$$

$$\xi_{k-1}-\epsilon_k\sin\xi_{k-1}=n_k^{-3}t_{k-1}, \tag{17}$$

$$\xi_k-\epsilon_k\sin\xi_k=n_k^{-3}t_k=n_k^{-3}(t_{k-1}+T_T),$$

$$q_k=n_k^2(1-\epsilon_k\cos\xi_k),$$

$$p_k=\frac{n_k}{q_k}\epsilon_k\sin\xi_k,$$

where $n_k=(2|E_k|)^{-1/2}$ is the classical principal action (directly related to the principal quantum number) and $\epsilon_k=\sqrt{1+2E_k\Lambda^2}=1$ is the eccentricity. For $E_k>0$, M becomes correspondingly

$$q_{k-1}=n_k^2(\epsilon_k\cosh\xi_{k-1}-1),$$

$$p_{k-1}+\Delta p=\frac{n_k}{q_{k-1}}\epsilon_k\sinh\xi_{k-1},$$

$$\epsilon_k\sinh\xi_{k-1}-\xi_{k-1}=n_k^{-3}t_{k-1}, \tag{18}$$

$$\epsilon_k\sinh\xi_k-\xi_k=n_k^{-3}t_k=n_k^{-3}(t_{k-1}+T_T),$$

$$q_k=n_k^2(\epsilon_k\cosh\xi_k-1),$$

$$p_k=\frac{n_k}{q_k}\epsilon_k\sinh\xi_k.$$

The kicked one-dimensional (1D) atom represents a time-dependent dynamical system with one degree of freedom. It can be canonically transformed into an equivalent time-independent system with two degrees of freedom (usually referred to as a 1 and 1/2 degrees of freedom system [23]).

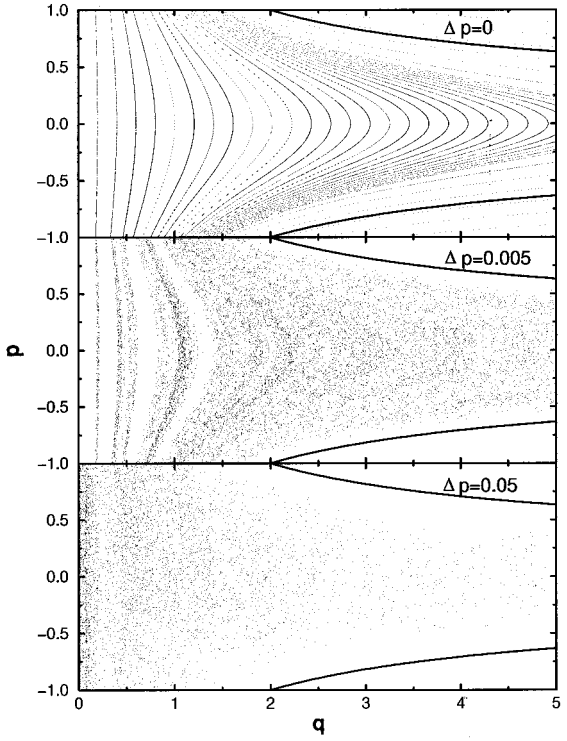

FIG. 4. Poincaré surface of section for the 1D kicked hydrogen atom for $\nu_T=(2\pi)^{-1}$ and various positive Δp values. The thick line indicates the separatrix between bound and continuum unperturbed tori.

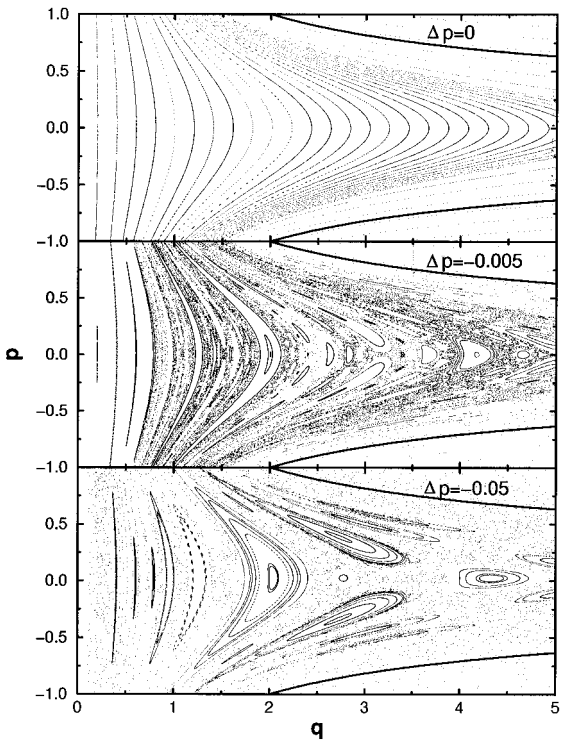

FIG. 5. Poincaré surface of section for the 1D kicked hydrogen atom for $\nu_T=(2\pi)^{-1}$ and various negative Δp values. The thick line indicates the separatrix between bound and continuum unperturbed tori.

This low dimensionality greatly simplifies the study of the electronic dynamics. Regular and chaotic dynamics can be easily identified by the Poincaré surface of sections. Because the Hamiltonian is periodic in time, Poincaré sections (of the equivalent time-independent system) can be generated by taking stroboscopic snapshots of (q,p) during every period of the perturbation. If the dynamics is regular (i.e., if there exists a constant of motion), a phase-space trajectory is constrained to a torus whose image on a section takes the form of a closed loop.

Figures 4 and 5 display Poincaré surfaces of sections of the kicked 1D atom for $\Delta p>0$ and $\Delta p<0$, respectively. For $\Delta p=0$ the dynamics is fully regular and each of the tori in the figure corresponds to a different $H_{\rm at}^{\rm 1D}=$ const surface. Due to the Coulomb singularity at the origin $(q=0)$, this dynamical system features several nonstandard properties; for example, the unperturbed tori do not have the appearance of closed loops within any finite domain in phase space since $p\to\infty$ as $q\to 0$. Furthermore, as soon as the perturbation $\Delta p>0$ is turned on (momentum transfer in the direction of the apocenter), the tori are completely destroyed no matter how small Δp is, and the system becomes globally chaotic, in agreement with the predictions of Hillermeier *et al.* [6]. More surprisingly, for $\Delta p<0$ (kick toward the Coulomb force center), some of the tori survive weak perturbations. However, the transition to a mixed phase space with a sizable chaotic region occurs for an arbitrary small momentum transfer. All chaotic regions become immediately interconnected forming a chaotic sea. According to Eq. (16) this is due to the fact that the high momentum ''wing,'' $p\Delta p>E_k-(\Delta p)^2/2$, of any unperturbed tori becomes immediately destroyed. The coexistence of a chaotic sea and of tori determines the ionization dynamics. Note that stable regions of phase space are only associated with bound states of the unperturbed motion: i.e., $H_{\rm at}^{\rm 1D}<0$. (For reference, the torus $H_{\rm at}^{\rm 1D}=0$ separating bound and continuum unperturbed tori is also shown in the figures.)

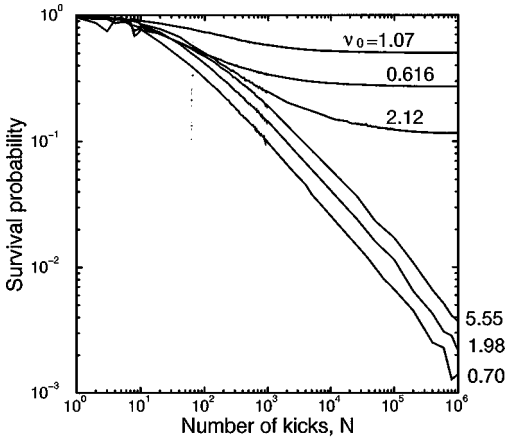

FIG. 6. Survival probability for the 1D kicked hydrogen atom at various scaled frequencies ν_0 as a function of the number of kicks.

Consider an atom in a well-defined n level (i.e., in a well-defined unperturbed torus defined by the initial binding energy). When subject to a train of impulses, ionization of such an atom occurs as soon as the unperturbed torus overlaps with the chaotic sea which, in turn, is connected with the continuum. On the other hand, the partial stability of the atom against ionization depends on whether or not the unperturbed torus overlaps with a stable region of phase space. Hillermeier *et al.* [6] found that the survival probability of atoms decays algebraically as a function of time for $\Delta p>0$, independent of the strength of the kicks and the frequency of the train. This is a consequence of the fully developed chaos in this system. In turn, Fig. 6 shows that for $\Delta p<0$ the survival probability as a function of the number of kicks, N, can be either dynamically stable or unstable depending on the pulse repetition frequency of the train. Therefore, the survival probability of an atom following ap-

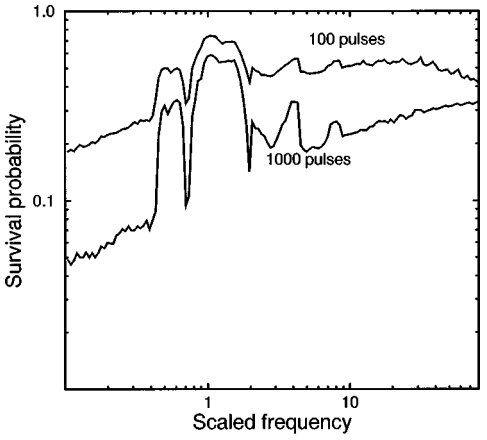

FIG. 7. Survival probability of a 1D kicked atom with initial energy $E=-0.5$ following application of 100 and 1000 kicks with $\Delta p=-0.3$ as a function of the pulse repetition frequency.

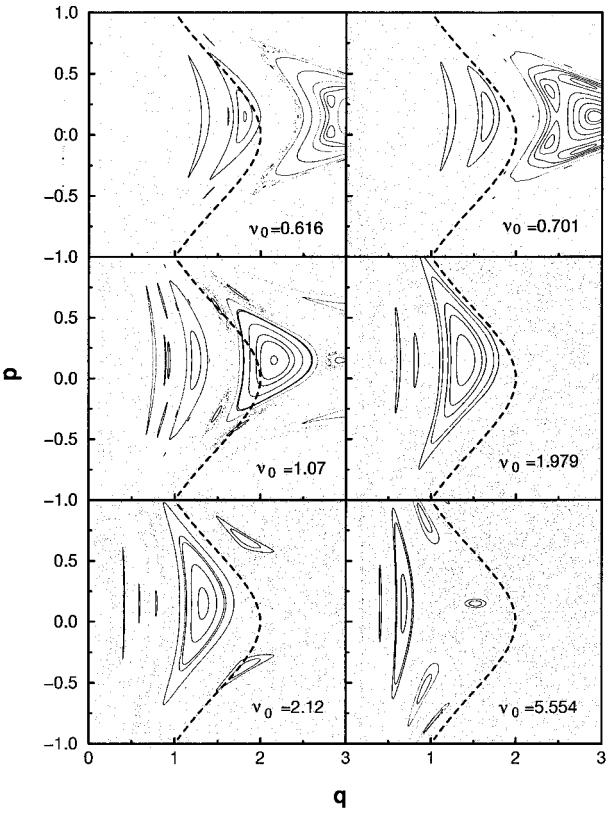

FIG. 8. Poincaré surface of sections for the 1D kicked hydrogen atom for $\Delta p=-0.3$ and various ν_T values. The dashed line indicates the unperturbed torus associated with the initial state of the atom in Fig. 9.

plication of a large number of kicks exhibits several pronounced peaks as a function of the repetition frequency (Fig. 7). In order to compute the probabilities in Figs. 6 and 7, a microcanonical ensemble of points in an unperturbed torus with energy $E=-0.5$ is followed as a function of time. The survival probability is given by the fraction of points which remain bound (i.e., $E<0$) after the train of pulses. Because of classical scaling invariance [Eqs. (2)–(6)], the survival probability is a function of the scaled variables $\Delta p_0=\Delta p/p_{n_i}, \nu_0=\nu/\nu_{n_i}$, where $p_{n_i}=n_i^{-1}$ and $\nu_{n_i}=(2\pi n_i^3)^{-1}$ only. Therefore, the results of Figs. 6 and 7 and in the following are presented in scaled units and are classically valid for any n_i initial level.

Each of the peaks in Fig. 7 is associated with a regular island in phase space. The survival probability is given by the fraction of the initial phase-space points that are contained within a given island. This is more clearly illustrated in Fig. 8, where we display Poincaré maps for different repetition frequencies together with the fixed initial torus. For repetition frequencies $\nu_T=0.616,1.07,2.12$, the initial torus overlaps with different stable islands and, therefore, stabilization is obtained by trapping the phase-space trajectories within a given island. In turn, for $\nu_T=0.701,1.978,5.554$, the initial torus lies in the chaotic sea and the atom becomes fully ionized.

Ionization does not necessarily happen immediately and, in fact, an electron may wander among various regions of phase space before reaching the continuum. This is illustrated in Fig. 9, where we display a Poincaré section of a single trajectory of an electron which is eventually ionized. The time evolution of the electron displays intermittency, periods of trapping near stable islands. However, since the residual tori are not confining, the trapping is only transient and the trajectory will eventually ''jump'' to another region of the chaotic sea and escape into the continuum.

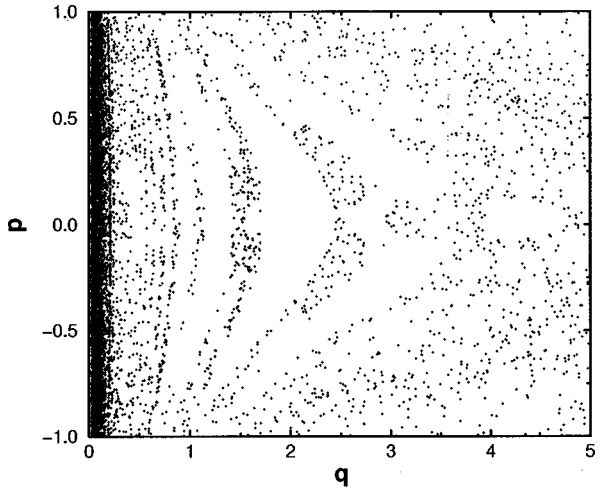

FIG. 9. Poincaré surface of section of a single trajectory starting in a chaotic region of phase space for the 1D kicked hydrogen atom for $\Delta p=-0.05$ and $\nu_T=1$.

The identification of the periodic orbits around which the stable islands are organized proceeds by noting that the binding energy must be unchanged following some integer number j of applied kicks, i.e.,

$$E_k=M^jE_{k-j}=E_{k-j}. \tag{19}$$

For a period-one ($j=1$) fixed point, Eqs. (19) and (16) imply

$$\frac{\Delta p^2}{2}+p\Delta p=0 \tag{20}$$

or $p=-\Delta p/2$, which agrees with the p coordinate of the center of the most prominent islands in Figs. 4, 5, and 8. The

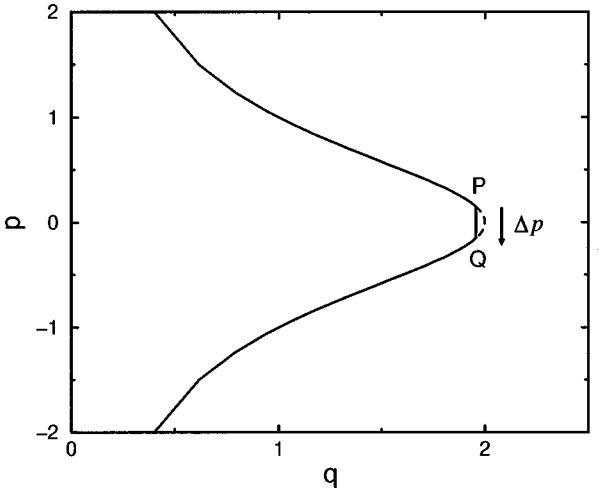

FIG. 10. Stable orbit for $\nu_T=1.25$ and $\Delta p=-0.3$. The dashed lines indicate the segment of the Coulomb orbit that is not reached by the electron.

periodic orbit which corresponds to the center of the largest stable island can be identified with the help of its projection onto the (q,p) plane, as shown in Fig. 10. The trajectory has been followed for several kicks involving segments of many Coulomb orbits having the same binding energy (i.e., the same unperturbed period).

According to Eq. (17), a kick maps a point $P=(q,p=-\Delta p/2)$ on a given Kepler ''orbit'' onto a point $Q=(q,p=\Delta p/2)$ of another orbit, as illustrated by the vertical arrow in Fig. 10. The subsequent unperturbed Coulomb evolution transports the point Q along the direction of the arrow back to point P, $M_{\mathrm{Coul}}(Q)\simeq P$. The periodic orbit is therefore nothing but a sequence of segments of full Coulomb orbits cut short by the kick. For this to occur, the time separation T_s between kicks (pulses) must be less than the Kepler period, i.e., $T_s=\alpha T_{n_i}$ with $\alpha<1$. Figure 7 suggests the existence of a family of stable periodic orbits with scaled frequencies $\nu_T^s=(\alpha+s)^{-1}$ $(s=0,1,2,\ldots)$ corresponding to orbits that complete s full periods and one segment α prior to the next kick, mapping P onto Q. From Eq. (16), the simple expression

$$\alpha=\pi^{-1}\left(\cos^{-1}\left[\frac{\Delta p^2-4}{\Delta p^2+4}\right]+\frac{4\Delta p}{\Delta p^2+4}\right) \tag{21}$$

can be obtained. Periodic orbits that are more complex than that in Fig. 10 also exist that involve transfer back and forth between several energy levels [20]. They are associated with tori that have undergone a bifurcation. The center of the torus overlapping the initial state of the electron for $\nu_T=2.12$ in Fig. 8 provides an example involving two energy levels [i.e., $j=2$ in Eq. (19)]. In this case a kick excites the electron to a higher energy level and, subsequently, another kick deexcites the electron back to its original level. The electronic motion becomes trapped within these two levels.

IV. THREE-DIMENSIONAL KICKED ATOM

In order to relate the results of the preceding section to the experimental data, it is necessary to analyze the extent to which the phase-space structure for the 1D system is preserved for the 3D kicked atom, especially since it is not obvious *a priori* that the stability properties should parallel each other. For a 1D system, tori are, in general, nested into each other and they are said to divide the phase space. The dynamics of chaotic orbits is constrained by regular islands of nested tori. This is not necessarily true for higher dimensions where the possibility of slow diffusion between stochastic layers enclosed by KAM-like tori exists (Arnold diffusion [23]). In this section we show that the dynamical stabilization in 1D closely mimics the stabilization in 3D. In particular, certain (but not all) classes of stable islands exist in both 1D and 3D. Moreover, because of the existence of the chaotic sea for the 1D kicked atom for any $\Delta p\neq 0$, the effect of the higher dimension does not fundamentally alter the chaotic pathway to ionization.

Consider the electron in a 3D hydrogen atom that is subject to a periodic train of impulses $\Delta\vec{p}=\Delta p\hat{z}$. The Hamiltonian for this problem is

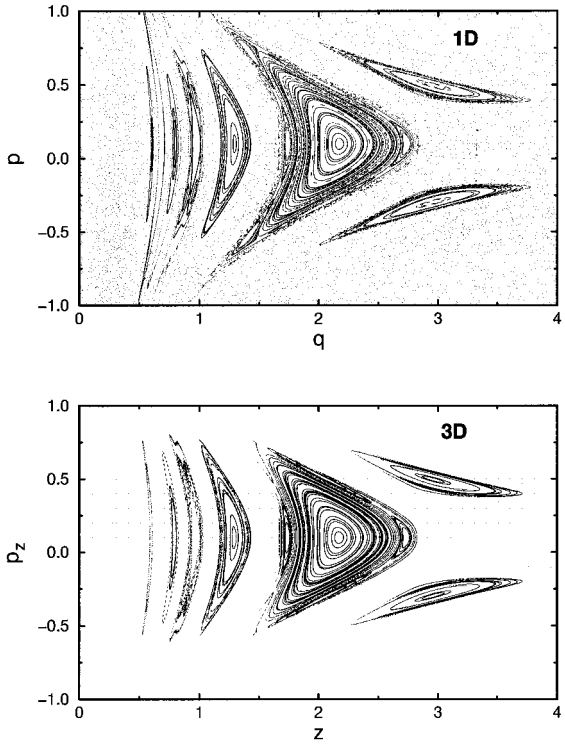

FIG. 11. Comparison of the Poincaré surfaces of sections for the 1D kicked hydrogen atom and the 3D kicked hydrogen atom ($L_z=2.510^{-4}$) subject to a train of pulses with $\Delta p=-0.2$ and $\nu_0=1$. The 3D section corresponds to $\rho=0.1$ and $p_\rho=0$.

$$H^{3\mathrm{D}}=H_{\mathrm{at}}-z\Delta p\sum_{j=1}^{N}\delta(t-j\nu_t^{-1}), \tag{22}$$

where the atomic Hamiltonian in cylindrical coordinates is given by

$$H_{\mathrm{at}}=\frac{p^2}{2}-\frac{1}{r}=\frac{p_z^2+p_\rho^2}{2}+\frac{L_z^2}{2\rho^2}-\frac{1}{\sqrt{z^2+\rho^2}} \tag{23}$$

with $\vec{L}=\vec{r}\times\vec{p}=(L_x,L_y,L_z)$ the angular momentum and $\rho^2=x^2+y^2$. Since the impulsive momentum transfer is along the $\hat{z}$ direction, L_z is a constant of motion and the kicked atom represents a time-dependent dynamical system with two degrees of freedom (i.e., a time-independent 2 and 1/2 degree of freedom system). M maps the four-dimensional phase space (ρ,z,p_ρ,p_z) onto itself.

Remarkably, calculations show that the stable islands for the 3D kicked atom mimic those for the 1D kicked system. This is illustrated in Fig. 11, in which Poincaré sections are compared. For the 3D case, the construction of the Poincaré surface requires, in addition to taking stroboscopic pictures, the slicing of phase space because of the higher dimensionality of the dynamical systems. In Fig. 11 we have taken slices of $(\rho\pm\Delta\rho),(p_\rho\pm\Delta p_\rho)$ near $\rho\sim 0.1$, $p_\rho\sim 0$, and $L_z=0$. Clearly, setting $\rho=0$, $p_\rho=0$, and $L_z=0$ in Eqs. (22) and (23) yields a Hamiltonian that is equivalent to the 1D Hamiltonian. Note, however, that because of the larger available phase space, chaotic trajectories in 3D are unlikely to return to the original slice of the Poincaré section after a

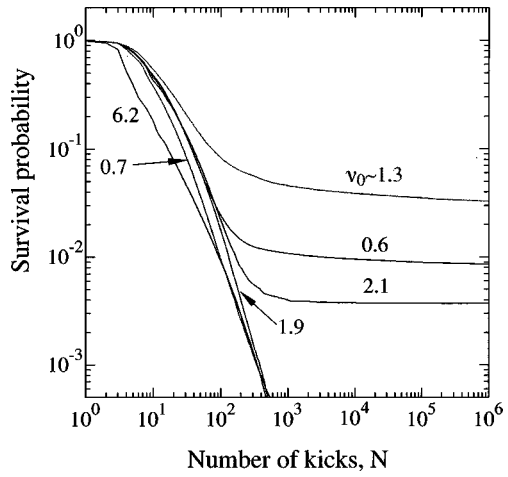

FIG. 12. Survival probability for the kicked hydrogen atom with $L_0=l_i/n_i=(388)^{-1}$ at various frequencies ν_0 as a function of the number of kicks.

finite number of kicks. The close correspondence between the Poincaré surface of sections in 1D and 3D in Fig. 11 is due to the fact that the phase-space slice taken near $\rho=0,p_\rho=0$ corresponds to regions in phase space that have large overlap with the extreme ''uphill'' or blueshifted parabolic states (i.e., uphill in the average field provided by the train of pulses).

Presently, Rydberg atoms are experimentally created by single photon excitation of alkali-metal atoms, leading to small initial quantum numbers l_i and m_i, and cannot be considered to be quasi-one-dimensional. Nevertheless, as shown in Fig. 12, dynamical stabilization can still occur at frequencies similar to those at which stabilization is expected for the 1D kicked atom. The reason is partly that the initial electronic state has a finite overlap with the extreme Stark states, which are associated with stable islands in Fig. 11. However, only a small fraction of the microcanonical ensemble of trajectories representing initial quantum numbers $n_i=388,l_i=1$ belong to these islands. There are, in addition, other stable islands that cannot be easily associated with a

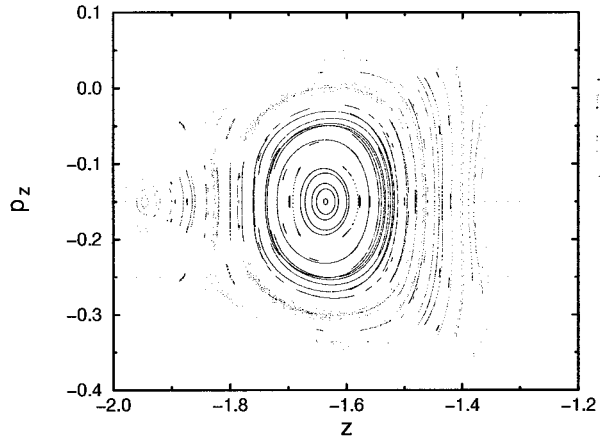

FIG. 13. Poincaré surface of section around the most stable region of phase space associated with the kicked hydrogen atom for $\nu_0=(2\pi)^{-1}$ and $\Delta p_0=0.2$ corresponding to $\rho=1.05,p_\rho=0$. Each trajectory has been followed for up to one million kicks.

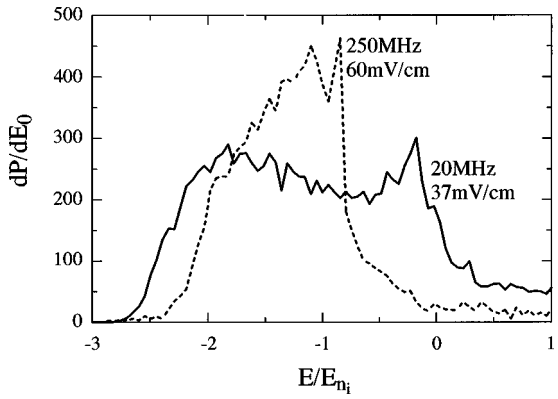

FIG. 14. Calculated final-state energy distribution following application of 50 HCPs with pulse repetition frequencies ν of 250 MHz and 20 MHz to K(388p) atoms. The pulse amplitudes are chosen to ionize ~90% of the parent atoms.

quasi-1D system. Figure 13 provides an example of such stable regions and corresponds to a cut at $\rho=1.05,p_\rho=0$. The identification of the periodic orbit at the center of the main stable island in the figure proceeds by noting that the binding energy must be unchanged following a kick, much like for the 1D system (i.e., $p_z=-\Delta p/2$). However, a simple physical picture of the periodic orbit is presently not available.

V. EXCITED BOUND-STATE DISTRIBUTION

Additional information on dynamical stabilization and chaotic evolution is contained in the distribution of excited bound states that remain following application of the HCP train. If dynamical stabilization occurs, the distribution of excitation energies of the surviving bound states should be sharply peaked at or near the initial energy. Conversely, chaotic dynamics should result in the population of states with a broad distribution in energy. Figure 14 shows the calculated final excited state, expressed as a function of the binding energy for HCP trains, one with $\nu_0\simeq 2.3$, corresponding to the region of partial dynamical stabilization, and one with $\nu_0\approx 0.18$, corresponding to the fully chaotic regime. In each case, the pulse amplitudes were such that ~90% of the parent atoms are ionized. In the absence of an applied HCP train, the energy distribution corresponds to a δ function at $E_0=E/E_{n_i}=1$ (i.e., atoms with well-defined initial n and, therefore, energy). After interaction with the HCP train, the final-state distribution is broadened and its width is determined by the overlap between the ensemble of perturbed tori near the stable island and the initial unperturbed torus. However, the distribution is significantly narrower in the regime where dynamical stabilization can occur than where ionization is fully chaotic. In the case of chaotic ionization, the remaining population is distributed over a broad range of states extending up to the ionization threshold.

Evidence of this behavior is contained in the experimentally measured SFI profiles. As shown in Fig. 15, in the absence of an applied HCP train, a single relatively narrow SFI profile is observed that corresponds to ionization of parent n atoms with well-defined initial energy. The SFI profile measured following application of a train of 50 HCPs with $\nu_0\sim 1.5$ and amplitude ~60 mV cm^{-1}, sufficient to ionize

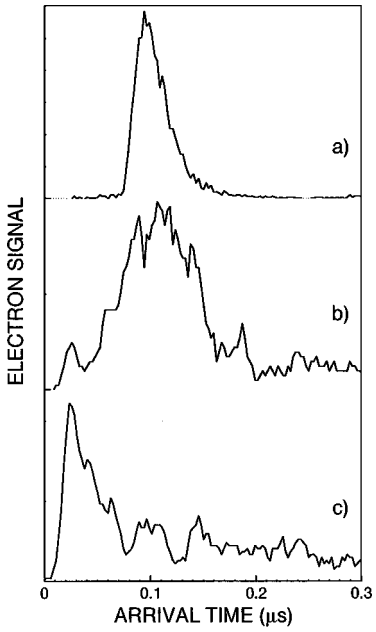

FIG. 15. SFI profiles observed for (a) parent K(np) atoms with $n \sim 388$, and following application of 50 HCPs with pulse repetition frequencies of (b) 166 MHz and (c) 20 MHz. The HCP amplitudes of ~ 60 mV cm^{-1} and ~ 36 mV cm^{-1}, respectively, are sufficient to ionize $\sim 90\%$ of the parent atoms. To better compare the shapes of the profiles, the SFI spectra are normalized to equal peak heights.

$\sim 90\%$ of the parent atoms, is also included in Fig. 15. Ionization is observed at field strengths both above and below those characteristic of parent state ionization, indicating that HCPs application populates a range of final n states. The population transfer, however, is asymmetric, with more atoms being transferred to states of lower n than of higher n: i.e., the increase in the relative area under the SFI profile is greater at field strengths above, rather than below, those characteristic of parent state ionization. The distribution of final n states is peaked at a value of n that is somewhat below, but close to, that of the parent atoms. This behavior is consistent with theoretical predictions and indicates that dynamical stabilization is occurring. Figure 15 also includes SFI data obtained following application of a train of 50 HCPs with $\nu_0 \sim 0.18$ and amplitude 36 mV cm^{-1}, sufficient to again ionize $\sim 90\%$ of the parent atoms. The SFI profile is broader than that observed at the higher HCP repetition frequency and, in particular, contains a greater relative contribution from the ionization of very-high-n atoms, which is a characteristic of chaotic ionization. However, inspection of the data reveals that there are comparable numbers of product atoms (as measured by the appropriate areas under the SFI profiles) with values of n above and below that of the parent atoms, which is again consistent with the theoretical predictions. (The sharp peak observed in the SFI profile at early times, i.e., small values of applied field, results because the threshold field for ionization scales as n^{-4}. As a consequence, ionization of the highest n atoms is compressed into a narrow range of applied fields, i.e., a narrow time range.)

VI. CONCLUSIONS

The present work demonstrates that very-high-n Rydberg atoms subject to a train of HCPs provide an excellent model system for investigating the behavior of periodically driven systems. The experimental data provide evidence for dynamical stabilization which is in accord with theoretical predictions for both 1D and 3D impulsively kicked atoms. The good agreement between experiment and full CTMC simulations employing realistic potentials and pulse shapes demonstrates that, for the range of fields and pulse repetition frequencies studied here, classical-quantum correspondence approximately holds and quantum corrections appear to be negligible. Quantum calculations for this stabilization process are currently underway.

Impulsively driven Rydberg atoms provide an opportunity to study the correspondence between classical and quantum mechanics from a new perspective. Experimentally, very precise studies are possible if the initial quantum state of the atoms is precisely known and the HCP trains are accurately controlled and characterized. This may allow identification of the possible breakdown of quantum-classical correspondence and of quantum modifications to irregular classical dynamics. An ideal candidate for such a study would be a ''downhill'' quasi-one-dimensional kicked atom which is classically fully chaotic. The strong similarities between the 1D and 3D kicked atoms indicate that classical-quantum correspondence could be first analyzed in 1D where accurate quantum calculations may be computationally feasible. Other future possibilities include the use of a ''chirped'' pulse train in which the time separation between adjacent HCPs is varied to better stay in phase with the motion of the electron as it moves to higher orbits, and the use of HCPs that alternate in sign. The latter have been used, for example, to model the behavior of atoms subject to intense electromagnetic radiation, and experimental measurements might provide new insights into intense field stabilization. Also, because by varying the pulse width and/or shape the harmonic content of the driving field can be varied, such measurements might have a bearing on the more general problem of atomic excitation by multifrequency ''colored'' fields.

ACKNOWLEDGMENTS

The experimental work was supported by the National Science Foundation and the Robert A. Welch Foundation. The theoretical work was funded by the Division of Chemical Sciences, Office of Basic Energy Sciences, U.S.D.O.E. under Contract No. DE-AC05-96OR22464, managed by Lockheed Martin Energy Research Corporation, and the National Science Foundation.

[1] See, e.g., H. Schuster, *Deterministic Chaos* (VCH Publishers, Weinheim, 1988).

[2] A. Dhar, M. Nagaranjan, F. Izrailev, and R. Whitehead, J. Phys. B **16**, L17 (1983).

[3] A. Carnegie, J. Phys. B **17**, 3435 (1984).

[4] T. Grozdanov and H. S. Taylor, J. Phys. B **20**, 3683 (1987).

[5] J. Burgdörfer, Nucl. Instrum. Methods Phys. Res. B **42**, 500 (1989).

[6] C. F. Hillermeier, R. Blümel, and U. Smilansky, Phys. Rev. A **45**, 3486 (1992).
[7] M. Melles, C. O. Reinhold, and J. Burgdörfer, Nucl. Instrum. Methods Phys. Res. B **79**, 109 (1993).
[8] G. Casati, I. Guarneri, and G. Mantica, Phys. Rev. A **50**, 5018 (1994).
[9] H. Wiedermann, J. Mostowski, and F. Haake, Phys. Rev. A **49**, 1171 (1994).
[10] R. Jensen, Nature (London) **355**, 311 (1992).
[11] P. Koch and K. Van Leeuwen, Phys. Rep. **255**, 289 (1995).
[12] F. Moore, J. Robinson, C. Bharucha, P. Williams, and M. Raizen, Phys. Rev. Lett. **73**, 2974 (1994).
[13] S. A. Gardiner, J. I. Cirac, and P. Zoller, Phys. Rev. Lett. **79**, 4790 (1997).
[14] R. R. Jones, D. You, and P. H. Bucksbaum, Phys. Rev. Lett. **70**, 1236 (1993).
[15] C. O. Reinhold, M. Melles, H. Shao, and J. Burgdörfer, J. Phys. B **26**, L659 (1993).
[16] M. T. Frey, F. B. Dunning, C. O. Reinhold, and J. Burgdörfer, Phys. Rev. A **53**, R2929 (1996).
[17] M. Gavrila, in *Atoms in Intense Laser Fields*, edited by M. Gavrila (Academic Press, San Diego, 1992), p. 435.
[18] R. M. Potvliege and R. Shakeshaft, in *Atoms in Intense Laser Fields*, edited by M. Gavrila (Academic Press, San Diego, 1992), p. 373.
[19] K. C. Kulander, K. J. Schafer, and J. Krause, in *Atoms in Intense Laser Fields*, edited by M. Gavrila (Academic Press, San Diego, 1992), p. 247.
[20] C. O. Reinhold, J. Burgdörfer, M. T. Frey, and F. B. Dunning, Phys. Rev. Lett. **79**, 5226 (1997).
[21] L. D. Landau and E. M. Lifshitz, *Mechanics* (Pergamon Press, Oxford, 1960).
[22] R. Abrines and I. C. Percival, Proc. Phys. Soc. London **88**, 861 (1966); **88**, 873 (1966); I. C. Percival and D. Richards, Adv. At. Mol. Phys. **11**, 1 (1975); R. E. Olson, Phys. Rev. A **24**, 1726 (1981).
[23] G. M. Zaslavsky, R. Z. Sagdeev, D. A. Usikov, and A. A. Chernikov, *Weak Chaos and Quasi-Regular Patterns* (Cambridge University Press, New York, 1991).